Exposure-Effect Relationships in Established Rat Adjuvant-Induced and Collagen-Induced Arthritis: A Translational Pharmacokinetic-Pharmacodynamic Analysis

Harvey Wong, Lichuan Liu, Wenjun Ouyang, Yuzhong Deng, Matthew R. Wright and Cornelis E.C.A. Hop

Department of Drug Metabolism and Pharmacokinetics (HW, LL, YD, MRW, CECAH) and

Department of Immunology (WO), Genentech Inc., South San Francisco, CA.

Running title: Translational PK-PD Analysis of Rat Arthritis Models

Author to whom correspondence should be addressed:

Harvey Wong, PhD
Faculty of Pharmaceutical Sciences, The University of British Columbia
2405 Wesbrook Mall, Vancouver, BC, Canada, V6T 1Z3
Phone: 604-822-4707
Fax: 604-822-3035
E-mail: harvey.wong@ubc.ca

Number of pages: 47

Number of Tables: 2

Number of Figures: 8

Number of References: 30

Number of Words in Abstract: 242

Introduction: 780

Discussion: 1448

List of abbreviations: *%inh_score*: percent inhibition of the ankle histopathology score *; AD*:

ankle diameter**;** *,AD_initial*: initial ankle diameter on day 0; AHSS: ankle histopathology summed

scored; AIA: adjuvant-induced arthritis; AUC_{ankle}: area under the ankle diameter time profile; *C*:

concentration; CIA: collagen-induced arthritis; C_{ss}: steady-state concentration; E_{max}: maximum

%inh_score; EC_{50}: concentration of at which the *%inh_score* is at ½ the maximum value; *E*:

constant describing a linear component of the relationship between concentration and *%inh_score*;

k_{in}: rate of increase in ankle diameter; *I*: constant that relates the test agent concentration with

I_{AS}; IC_{50}: concentration of the test agent where I_{AS} is 50% of I_{max}; I_{AS}: rate constant describing the

reduction of ankle swelling by the drugs used in the AIA and CIA studies; I_{max}: maximum value

of I_{AS}.

Recommended Section Assignment: Drug Discovery and Translational Medicine

ABSTRACT

The ability of rodent immune-mediated arthritis models to quantitatively predict therapeutic activity of anti-arthritis agents is poorly understood. Two commonly used preclinical model of arthritis are adjuvant-induced arthritis (AIA) and collagen-induced arthritis (CIA) in rats. The objective of the current study is to investigate the relationship between efficacy in AIA and CIA in rats, and clinical efficacy in rheumatoid arthritis patients using translational PK-PD analysis. A range of doses of indomethacin (a nonsteroidal anti-inflammatory drug), and three disease-modifying anti-rheumatic drugs (DMARD), methotrexate, etanercept, and tofacitinib, were evaluated in AIA and CIA rats. Dexamethasone was included in this study as a positive control. Ankle diameter AUC (AUC_{ankle}) and ankle histopathology summed scores (AHSS) were used as efficacy endpoints for activity against disease symptoms (joint inflammation) and disease progression (joint damage), respectively. Translational PK-PD analysis was performed to rank-order preclinical efficacy endpoints at clinically relevant concentrations. For each drug tested, inhibition of both AUC_{ankle} and AHSS scores were generally comparable in both magnitude and rank order. Overall, based on both AUC_{ankle} and the AHSS inhibition, the rank ordering of preclinical activity for the DMARDs evaluated was tofacitinib > etanercept ≥ methotrexate. This ranking of preclinical efficacy was consistent with reported clinical efficacy. Of interest, indomethacin showed equal or often better efficacy than the three DMARDs evaluated on inhibiting AHSS despite having limited ability to prevent joint damage clinically in patients. The translational value of performing PK-PD analysis of arthritis models in rats is discussed.

INTRODUCTION

High attrition rates plague the drug discovery and development process with Phase II clinical trial success rates being <20% (Arrowsmith and Miller, 2013). By far, the most prominent reason for failure is lack of efficacy (>50% for both Phase II and Phase III) highlighting a need for to improve the predictability of "preclinical disease models" used aid in the identification of drug candidates. Rheumatoid arthritis (RA) is a chronic debilitating autoimmune disorder causing inflammation of many joints including those of the hands and feet. Finding treatments for RA remains a challenge as it is heterogeneous in nature and the biological mechanisms causing the disease are not well understood (Kollias et al., 2011). Rodent models of immune mediated arthritis remain a common and valuable approach for evaluation of mechanisms of inflammatory joint disease and relative efficacy of anti-arthritic agents (Kannan et al., 2005; Hegen et al., 2008; Bolon et al., 2011; Caplazi et al., 2015). Qualitatively, these models have characteristics that display both similarities and difference to RA in patients. Two of the most commonly used rodent models to evaluate existing or investigative therapies for rheumatoid arthritis are adjuvant-induced arthritis (AIA) and collagen-induced arthritis (CIA) in rats (Hegen et al., 2008; Bolon et al., 2011).

The first model of rheumatoid arthritis described was AIA in rats (Pearson, 1956). AIA is induced by a single injection of complete Freund adjuvant in Lewis rats and characterized by rapid disease onset, severe polyarticular inflammation, bone resorption and perosteal bone proliferation. Disease progression onset occurs 10 days after adjuvant injection and usually lasts less than one month. AIA in rats is a T-cell and neutrophil dependent disease that is complement independent, and has no documented role for B-cells (Hegen et al., 2008). Similar to human disease, AIA results in swelling and loss of function of joints, cartilage damage, and lymphocyte

infiltration. However, bone resorption is more prominent in AIA rats compared to both CIA rats

and human RA. In addition, unlike human RA, the gastrointestinal and genitourinary tracts, the

skin, and the eyes are affected in AIA.   CIA in rats was first described by Trentham and

coworkers (Trentham et al., 1977) and has similarity to human rheumatoid arthritis in that

females are more susceptible to arthritis in this model. Arthritis onset is rapid, usually

developing 10–13 days after immunization with homologous or heterologous type II collagen,

peaking at about days 15-20 and then gradually declining. The resulting polyarthritis is

characterized by marked cartilage destruction associated with immune complex deposition on

articular surfaces, bone resorption, periosteal proliferation, and moderate to marked synovitis and

periarticular inflammation (Bendele, 2001). Collagen-specific T and B cells are both required for

disease induction, and CIA can be transferred with serum from diseased animals into recipient

strains. Rat CIA differs from human RA in that it is self-limiting and not characterized by

exacerbations and remissions. Further, the inflammatory cell infiltrate in rat CIA consists

predominantly of polymorphonuclear cells, whereas a high proportion of mononuclear cells are

seen in human RA (Hegen et al., 2008). CIA in rats differs from AIA in that in that it is less

severe, complement dependent, and there is involvement of B-cells. Despite the broad use of

AIA and CIA rats for the evaluation of new RA therapies, there has been no detailed

characterization of drug concentration-effect relationships limiting the understanding of the

translatability of findings in these preclinical models to humans.

Preclinical pharmacokinetic-pharmacodynamic (PK-PD) analysis can play an important role

in the drug discovery and development process by providing an integrated assessment of the

relationships between drug concentrations in the body and efficacy (Liu, 2011, Wong et al., 2012a,

Wong et al., 2012b; Shuck et al., 2015; Wong et al., 2017). In particular, PK-PD analysis allows for

the quantitative translation of species differences in pharmacokinetics and/or in vivo drug potency.

The primary objective of the current study was to perform a detailed PK-PD analysis of the effect of

drugs commonly used to treat RA in therapeutic AIA and CIA rats. The PK-PD analysis will

provide a detailed understanding of drug concentration-effect relationships and facilitate translation

of preclinical efficacy in therapeutic AIA and CIA rats to clinical efficacy. Such information is

currently lacking making it difficult to understand how the performance of new drug candidates in

these efficacy models will translate to clinical efficacy in rheumatoid arthritis patients. The four

drugs tested were indomethacin (a nonsteroidal anti-inflammatory drug [NSAID]), methotrexate (a

standard of care disease-modifying anti-rheumatic drug [DMARD]), etanercept (an anti-TNF

biologic), and tofacitinib (a recently approved oral Janus kinase [JAK] inhibitor). Dexamethasone

(a corticosteroid) which is delivered in humans by local injection was included as it serves as a

common positive control in both preclinical models.

MATERIALS AND METHODS

Adjuvant-Induced Arthritis (AIA)

Efficacy: Male Lewis rats (Charles River Laboratories, Wilmington, MA) weighing 204-262 grams (average weight = 230 grams) were used for AIA studies. Rats (n= 8 per group for arthritis efficacy groups; n=4 per group for normal control rats; and n=3 per group for supporting pharmacokinetic satellite groups) were anesthetized with isoflurane and injected with 100 µl of Freund's Complete Adjuvant (Sigma-Aldrich, St. Louis, MO) containing lipoidal amine (60 mg/ml, Bolder BioPATH, Inc., Boulder, CO) at the base of the tail on day 0. On study days 8–9, onset of arthritis occurred. Ankle caliper measurements were made with a Digitrix II micrometer (Fowler & NSK). On study day 9 (day 1 of established disease), rats were randomized into treatment groups with each group having balanced mean ankle diameters. Randomization was performed after ankle joint swelling was established and there was good evidence of bilateral disease. Rats with outlier ankle measurements (i.e., low or high scores) were kept for supporting pharmacokinetic (PK) satellite groups. Dosing was initiated upon enrollment (day 1 of established disease), and the doses and dosing regimen of various test agents is indicated in Table 1. Animals in the main efficacy groups were euthanized following end of study on day 8 of established disease. Area under the ankle diameter time profile (AUC_{ankle}) for each treatment group was determined using the trapezoid rule (Gibaldi and Perrier, 1982). Percent inhibition of AUC_{ankle} was determined using equation 4 as described below in the PK-PD Analysis of Ankle Swelling section. This basic study design and animal usage was approved by Bolder BioPATH's Institutional Animal Care and Use Committee (IACUC) for compliance with regulations prior to study initiation.

Pharmacokinetics: Supporting pharmacokinetic information the AIA studies was gathered at doses (n=3 rats per group) covering the range of doses used for each agent used (see Table 1). AIA rats in the PK satellite groups were dosed similarly to the main efficacy groups and whenever possible pharmacokinetic assessments were taken on the last day of study (day 7 of established disease). The pharmacokinetic assessment for the high dose groups for indomethacin (6 mg/kg) was taken following the first dose on day 1 of established disease due to potential tolerability concerns at these doses. Etanercept pharmacokinetic assessments were made on both day 1 and day 7 of established disease to assess any potential changes in etanercept exposure following multiple doses resulting from anti-therapeutic antibodies. On the day of the pharmacokinetic assessment plasma (indomethacin, methotrexate, tofacitinib, dexamethasone) or serum (etanercept) samples were taken at 0.25, 0.5, 1, 3, 6, 9, 12 and 24 hours post-dose. Plasma/serum samples were stored frozen until concentrations were assessed. The concentrations of indomethacin (Sigma-Aldrich, St. Louis, MO), methotrexate (Sigma-Aldrich, St. Louis, MO), tofacitinib (Genentech, South San Francisco, CA), and dexamethasone (Vedco Inc., Saint Joseph, MO) in plasma were determined by LC/MS/MS. Etanercept (Amgen, Thousand Oaks, CA) serum concentrations were determined by enzyme-linked immunosorbent assays. Rats used for pharmacokinetic assessment were euthanized after the final 24 hour sampling on day 1 or 7. Estimated pharmacokinetic parameters for AIA rats are shown in Supplemental Table 6.

Ankle Histopathology: Preserved and decalcified (5% formic acid) ankle joints were cut in the sagittal plane into 2 approximately equal halves and processed for paraffin embedding, sectioned, and stained with Toluidine Blue. Tissues were examined microscopically, and adjuvant arthritic ankles are given scores of 0-7 for inflammation, bone resorption, cartilage

damage and pannus where a score of 0 represents normal with increasing numbers representing increasing severity of disease. Detailed description of criteria for scores is listed in Supplemental Table 1. Summed inflammation, pannus, bone and cartilage scores were derived and group means compared using a one-way analysis of variance (ANOVA) with significance set at $p < 0.05$.

Collagen-Induced Arthritis (CIA)

Efficacy: Female Lewis rats (Charles River Laboratories, Wilmington, MA) weighing 156-189 grams (average weight = 172 g) were used for CIA studies. Rats (n= 8 per group for arthritis efficacy groups; n=4 per group for normal control rats; and n=3 per group for supporting pharmacokinetic satellite groups) were anesthetized with isoflurane and injected with 300 µl of Freund's Incomplete Adjuvant (Difco, Detroit, MI) containing 2 mg/ml bovine type II collagen (Elastin Products, Owensville, Missouri) at the base of the tail and at 2 sites on the back on days 0 and 6. Ankle caliper measurements were made with a Digitrix II micrometer (Fowler & NSK). By study day 10 (day 1 of established disease), onset of arthritis occurred and rats were randomized into treatment groups with each group having balanced mean ankle diameters. Randomization was performed after ankle joint swelling was established and there was good evidence of bilateral disease. Rats with outlier ankle measurements (i.e., low or high scores) were kept for supporting pharmacokinetic (PK) satellite groups (see below). Dosing was initiated upon enrollment (day 1 of established disease), and the doses and dosing regimen of various test agents is indicated in Table 1. Animals in the main efficacy groups were euthanized following the end of study on day 8 of established disease. AUC_{ankle} and percent inhibition of AUC_{ankle} was as described for the AIA model above. This basic study design and animal usage

was approved by Bolder BioPATH's Institutional Animal Care and Use Committee (IACUC) for compliance with regulations prior to study initiation.

Pharmacokinetics: Supporting pharmacokinetics for CIA studies were evaluated in a similar manner as described for the AIA studies above. Estimated pharmacokinetic parameters for CIA rats are shown in Supplemental Table 6.

Ankle Histopathology: Preserved and decalcified (5% formic acid) ankle joints were cut in half longitudinally, processed through graded alcohols and a clearing agent, infiltrated and embedded in paraffin, sectioned, and stained with Toluidine Blue. The tissues were examined microscopically. Collagen arthritic ankles were given scores of 0-5 for inflammation, pannus formation, cartilage damage and bone resorption where a score of 0 represents normal with increasing numbers representing increasing severity of disease. A detailed description for scores is listed in Supplemental Table 2.

Pharmacokinetic-Pharmacodynamic (PK-PD) Analysis

Pharmacokinetic Analysis: Pharmacokinetic parameters for each test agent in rats from pharmacokinetic satellite groups were estimated using SAAM II (Saam Institute, University of Washington, Seattle, WA). Estimated parameters were used to simulate systemic concentrations of test agents for the various doses/ regimens in the AIA and CIA studies described below during the PK-PD modeling process of ankle swelling.

PK-PD Analysis of Ankle Swelling: The PK-PD analysis of ankle swelling was a naïve averaged analysis. Briefly, longitudinal ankle diameter data for each dose level from the AIA and CIA

efficacy studies was averaged. The longitudinal average ankle diameter values were fitted to an

indirect response model (Figure 1A) as described by the following differential equation.

$$\frac{d(AD)}{dt} = k_{in} - I_{AS}(AD - AD_{initial})$$ (Equation 1)

AD (inches) is defined as the ankle diameter, $AD_{initial}$ (inches) is the initial ankle diameter on day

0, t (day) is time, k_{in} (inches×day^{-1}) is the rate of increase in ankle diameter, and I_{AS} (day^{-1}) is the

rate constant describing the reduction of ankle swelling by the drugs used in the AIA and CIA

studies.

For studies where the anti-ankle swelling effect of the agent of interest was saturable, I_{AS} was

defined by Equation 2.

$$I_{AS} = \frac{I_{max} \times C}{IC_{50} + C}$$ (Equation 2)

I_{max} (day^{-1}) is defined as the maximum value of I_{AS}, C is the concentration of the test agent, and

IC_{50} is the concentration of the test agent where I_{AS} is 50% of I_{max}.

For studies where the anti-ankle swelling effect was linear, I_{AS} was defined by Equation 3:

$$I_{AS} = I \times C$$ (Equation 3)

I ($\mu M^{-1} \times day^{-1}$) is defined as a constant that relates the test agent concentration with I_{AS}.

The choice of using a saturable effect (Equation 2) versus a linear effect (Equation 3) was based on reduction of fitting statistics such as the objective function, Akaike information criterion, and the Schwarz-Bayesian information criterion. Both models assume that drug action works to decrease the rate of increase of ankle swelling which is consistent to what is known about the drugs that are modeled. Pharmacodynamic parameters are presented as the estimate followed by the coefficient of variation (CV) in parentheses (Supplemental Table 3). Species differences in plasma protein binding were not considered in the PK-PD analysis as plasma protein binding of the drugs evaluated were comparable based on published literature.

Simulations of clinical regimens/exposures were performed using the PK-PD model and pharmacodynamic parameter estimates from AIA and CIA studies in combination with human pharmacokinetic parameters obtained from the literature (see Supplemental Table 4) as described in Figure 1B. As we are quantitatively evaluating the clinical translatability of AIA and CIA efficacy to clinical activity in patients, the PD parameters estimated from AIA and CIA studies were used in the clinical simulations. In the simulations, clinically relevant doses and pharmacokinetics were used to simulate the effect of each test agent on the area under the ankle diameter time profile (AUC_{ankle}). AUC_{ankle} for mean ankle diameter vs time data from vehicle and treatment groups were determined using the trapezoid rule (Gibaldi and Perrier, 1982) and were assessed from study day 1 to 8. Percent inhibition of AUC_{ankle} was determined using equation 4.

$$\%inhibition\_AUC_{ankle} = \frac{AUC_{vehicle} - AUC_{treatment}}{AUC_{vehicle} - AUC_{normal}} \times 100\% \qquad \text{(Equation 4)}$$

where *%inhibition_AUC$_{ankle}$* is the percent inhibition of AUC_{ankle}, $AUC_{vehicle}$ is the AUC_{ankle} for the vehicle control arthritic group, $AUC_{treatment}$ is the AUC_{ankle} for the treatment group, and AUC_{normal} is the AUC_{ankle} for the normal control group (i.e. rats without arthritis receiving vehicle).

PK-PD Analysis of Ankle Histopathology: Individual (i.e. inflammation, pannus, cartilage damage, bone resorption) or summed ankle histopathology scores for each treatment group were normalized to vehicle control scores and converted to a percent inhibition using Equation 5.

$$\%inh\_score = \left(100 - \frac{score}{score_{vehicle}} \right) \times 100\% \qquad \text{(Equation 5)}$$

where *%inh_score* is the percent inhibition of the ankle histopathology score, *score* is the histopathology score as described in the ankle histopathology section for AIA and CIA rats, and *score$_{vehicle}$* is the ankle histopathology score for vehicle control rats.

The relationship between the steady-state concentrations of each agent tested and individual or summed ankle histopathology scores in rat CIA or AIA were defined by fitting ankle histopathology score vs concentration data to either a standard E_{max} equation (Equation 6) or an E_{max} equation with a linear effect component (Equation 7).

$$\%inh\_score = \frac{E_{max} \times C_{ss}}{EC_{50} + C_{ss}} \qquad \text{(Equation 6)}$$

$$\%inh\_score = \frac{E_{max} \times C_{ss}}{EC_{50} + C_{ss}} \times EC_{ss} \qquad \text{(Equation 7)}$$

where E_{max} is the maximum *%inh_score*, EC_{50} is the concentration of at which the *%inh_score* is at ½ the maximum value, E is a constant describing a linear component of the relationship between concentration and *%inh_score*, and C_{ss} is the steady-state concentration.   Steady-state concentrations for each dose level in rat AIA and CIA studies were determined by dividing steady-state AUC of the drug concentration-time profile by the dosing interval. In cases where supporting pharmacokinetic data was not collected for a specific treatment group, linear interpolation was performed to estimate a C_{ss}. This was performed with reasonable confidence as supporting pharmacokinetic data was gathered for treatment groups that were chosen to specifically cover the entire range of doses (see Table 1). The choice of using an E_{max} equation with (Equation 7) or without (Equation 6) a linear effect component was determined by selection of the particular equation that best minimized the sum of squares of residuals and the standard error of parameter estimates. Fitting of data from AIA or CIA studies was performed using for GraphPad Prism V4.02 (GraphPad Software Inc., San Diego, CA). Estimated pharmacodynamic parameters for ankle histopathology summed scores (AHSS) are presented in Supplemental Table 5.

Following fitting of the ankle histopathology score vs concentration data from AIA and CIA studies, percent inhibition of ankle histopathology scores at clinically active concentrations of the various test agents was determined. In brief, estimated parameters from fitting of ankle histopathology-concentration data were fixed, clinically relevant steady-state concentrations for each test agent were obtained from literature (see Table 2), and equations 6 or 7 were used to interpolate the %inh_score at the clinically relevant steady-state concentrations. Analysis of individual histopathology scores in rat CIA or AIA provided nearly identical conclusions to analysis

of summed ankle histopathology scores. Therefore, only the analysis of AHSS is presented in this

manuscript.

RESULT

Characterization of Dose-Efficacy Relationship in Preclinical Rat Arthritis Models

A range of doses of indomethacin, methotrexate, etanercept, tofacitinib, and dexamethasone were administered to AIA and CIA rats with established disease. Normal control rats treated with vehicle were included in all studies but showed no appreciable change in ankle diameter over the course of the study (Figures 2-6). The detailed results of these studies are described in the following sections for each drug.

Indomethacin: AIA – Figure 2A is a representative ankle diameter vs time plot for diseased animals treated with indomethacin (vehicle, 0.1, 0.3, 1, 3, and 6 mg/kg PO) on days 1 to 7 of established disease. Daily ankle diameter measurements were significantly ($p < 0.05$) reduced toward normal for AIA rats given 0.1 mg/kg (days 5 to 8), 0.3 mg/kg (days 3 to 8), 1 mg/kg (days 3 to 8), and 3 mg/kg (days 2 to 8) of indomethacin when compared to vehicle control rats. AIA rats treated with 6 mg/kg of indomethacin had significantly ($p < 0.05$) reduced ankle diameter measurements (on days 2 to 5) prior to being euthanized on day 5 due to intolerability. AUC_{ankle} was significantly ($p < 0.05$) and dose responsively reduced toward normal for AIA rats treated with 0.1 mg/kg (22% reduction), 0.3 mg/kg (46% reduction), 1 mg/kg (59% reduction), and 3 mg/kg (66% reduction) indomethacin when compared to vehicle controls. AUC_{ankle} was not determined for the 6 mg/kg dose as the dose was tolerated only until day 5. Indomethacin treatment resulted in a dose dependent decrease in ankle histopathology scores in AIA rats (see Figure 2B). All individual ankle histopathology parameters (inflammation, pannus, cartilage damage, bone resorption) were significantly ($p < 0.05$) reduced relative to the vehicle control for AIA rats treated with 3 and 6 mg/kg of indomethacin. AIA rats treated with 1 mg/kg Indomethacin had significantly ($p < 0.05$) reduced ankle inflammation

18

(44% reduction), cartilage damage (41% reduction), and bone resorption (54% reduction). At 0.3 mg/kg, only the decrease in ankle inflammation (30%) was significant. Accordingly, the effect of indomethacin on summed ankle histopathology scores relative to the vehicle control AIA rats was dose dependent across the entire range of doses tested, and significant ($p<0.05$) at doses of 1 (47% reduction), 3 (66% reduction) and 6 mg/kg (86% reduction) of indomethacin.

CIA – Figure 2C is a representative ankle diameter vs time plot for diseased animals treated with indomethacin (vehicle, 0.1, 0.3, 1, 3, and 6 mg/kg PO) on days 1 to 7 of established disease. Daily ankle diameter measurements were significantly ($p<0.05$) reduced toward normal for CIA rats given 0.1 mg/kg (days 4 to 8), 0.3 mg/kg (days 2 to 8), 1 mg/kg (days 2 to 8), and 3 mg/kg (days 2 to 8) of indomethacin when compared to vehicle control rats. CIA rats treated with 6 mg/kg of indomethacin had significantly ($p<0.05$) reduced ankle diameter measurements (on days 2 to 5) prior to being euthanized on day 5 due to intolerability. AUC_{ankle} was significantly ($p<0.05$) and dose responsively reduced toward normal for CIA rats treated with 0.1 mg/kg (25% reduction), 0.3 mg/kg (46% reduction), 1 mg/kg (66% reduction), and 3 mg/kg (92% reduction) indomethacin when compared to vehicle controls. AUC_{ankle} was not determined for the 6 mg/kg dose as the dose was tolerated only until day 5. Indomethacin treatment resulted in a dose dependent decrease in ankle histopathology scores in CIA rats (see Figure 2D). All individual ankle histopathology parameters (inflammation, pannus, cartilage damage, bone resorption) were significantly ($p<0.05$) reduced relative to the vehicle controls for CIA rats treated with 1, 3, and 6 mg/kg of indomethacin. CIA rats treated with 0.3 mg/kg indomethacin had significantly ($p<0.05$) reduced ankle pannus (54% reduction), and bone resorption (54% reduction). Accordingly, the effect of indomethacin on summed ankle histopathology scores relative to the vehicle control AIA rats was dose dependent and significant ($p<0.05$) at doses of 0.3 (39% reduction), 1 (55% reduction), 3 (85% reduction) and

19

6 mg/kg (96% reduction) of indomethacin. Effects of indomethacin were slightly more pronounced at similar doses in CIA rats when compared to AIA rats (Figure 2).

Methotrexate: AIA – Figure 3A is a representative ankle diameter vs time plot for diseased animals treated with methotrexate (vehicle, 0.1, 0.3, and 1 mg/kg PO) on days 1 to 7 of established disease. Daily ankle diameter measurements were significantly ($p<0.05$) reduced toward normal for AIA rats given 0.3 mg/kg (days 6 to 8) and 1 mg/kg (days 5 to 8). AUC_{ankle} was significantly ($p<0.05$) and dose responsively reduced toward normal for AIA rats treated with 0.3 mg/kg (14% reduction) and 1 mg/kg (27% reduction) methotrexate when compared to vehicle controls. Treatment with 1 mg/kg methotrexate to AIA rats resulted in significantly ($p<0.05$) reduced ankle inflammation (41% reduction) (see Figure 3B). The effect of methotrexate on summed ankle histopathology scores relative to the vehicle control AIA rats was significant ($p<0.05$) only at a dose of 1 mg/kg (28% reduction) of methotrexate.

    CIA – Figure 3C is a representative ankle diameter vs time plot for diseased animals treated with methotrexate (vehicle, 0.1, 0.3, and 1 mg/kg PO) on days 1 to 7 of established disease. No significant changes in daily ankle diameter measurements or AUC_{ankle} were observed. The effect of methotrexate on ankle histopathology scores in CIA rats is shown in Figure 3D. No significant effects of methotrexate on ankle histopathology were observed. Overall, methotrexate had less of an effect on CIA rats when compared to AIA rats.

Etanercept: AIA – Figure 4A is a representative ankle diameter vs time plot for diseased animals treated with etanercept (vehicle, 0.3, 1, 3, 10, and 30 mg/kg) by subcutaneous injection days 1, 4, and 7 of established disease. Daily ankle diameter measurements were significantly ($p<0.05$)

reduced toward normal for AIA rats given 1 mg/kg (days 6 to 8), 3 mg/kg (days 4 to 8), 10 mg/kg (days 4 to 8), and 30 mg/kg (days 4 to 8) of etanercept when compared to vehicle control rats. AUC_{ankle} was significantly ($p<0.05$) and dose responsively reduced toward normal for AIA rats treated with 1 mg/kg (14% reduction), 3 mg/kg (17% reduction), 10 mg/kg (20% reduction), and 30 mg/kg (24% reduction) etanercept when compared to vehicle controls. Etanercept treatment resulted in a dose dependent decrease in ankle histopathology scores in AIA rats (see Figure 4B). AIA rats treated with 10 mg/kg etanercept had significantly ($p<0.05$) reduced ankle inflammation (26% reduction). At 30 mg/kg, etanercept significantly reduced both ankle inflammation (25% reduction) and bone resorption (49% reduction). The effect of etanercept on summed ankle histopathology scores relative to the vehicle control AIA rats was dose dependent and significant ($p<0.05$) at doses of 10 (25% reduction) and 30 mg/kg (32% reduction) of etanercept.

CIA – Figure 4C is a representative ankle diameter vs time plot for diseased animals treated with etanercept (vehicle, 0.3, 1, 3, 10, and 30 mg/kg) by subcutaneous injection days 1, 4, and 7 of established disease. Daily ankle diameter measurements were significantly ($p<0.05$) reduced toward normal for CIA rats given 3 mg/kg (days 3 to 8), 10 mg/kg (days 2 to 8) and 30 mg/kg (days 2 to 8) of etanercept when compared to vehicle control rats. AUC_{ankle} was significantly ($p<0.05$) and dose responsively reduced toward normal for CIA rats treated with 3 mg/kg (37% reduction), 10 mg/kg (56% reduction), and 30 mg/kg (69% reduction) etanercept when compared to vehicle controls. Etanercept treatment resulted in a dose dependent decrease in ankle histopathology scores in CIA rats (see Figure 4D). All individual ankle histopathology parameters (inflammation, pannus, cartilage damage, bone resorption) were significantly ($p<0.05$) reduced relative to the vehicle controls for CIA rats treated with 30 mg/kg of etanercept. CIA rats treated with 10 mg/kg etanercept had significantly ($p<0.05$) reduced ankle pannus (61% reduction), cartilage damage (59%

reduction), and bone resorption (61% reduction). Accordingly, the effect of etanercept on summed ankle histopathology scores relative to the vehicle control AIA rats was dose dependent but significant ($p<0.05$) only at a dose of 30 mg/kg (66% reduction) of etanercept. Effects of etanercept were more pronounced in CIA rats when compared to AIA rats (Figure 4).

Tofacitinib: AIA – Figure 5A is a representative ankle diameter vs time plot for diseased animals treated with tofacitinib (vehicle, 0.5, 1.5, 5, 15, and 45 mg/kg PO) on days 1 to 7 of established disease. Daily ankle diameter measurements were significantly ($p<0.05$) reduced toward normal for AIA rats given 0.5 mg/kg (days 6 to 8), 1.5 mg/kg (days 3 to 8), 5 mg/kg (days 2 to 8), 15 mg/kg (days 2 to 8), and 45 mg/kg (days 2 to 8) of tofacitinib when compared to vehicle control rats. AUC_{ankle} was significantly ($p<0.05$) and dose responsively reduced toward normal for AIA rats treated with 1.5 mg/kg (19% reduction), 5 mg/kg (34% reduction), 15 mg/kg (47% reduction), and 45 mg/kg (66% reduction) tofacitinib when compared to vehicle controls. Tofacitinib treatment resulted in a dose dependent decrease in ankle histopathology scores in AIA rats (see Figure 5B). All individual ankle histopathology parameters (inflammation, pannus, cartilage damage, bone resorption) were significantly ($p<0.05$) reduced relative to the vehicle control for AIA rats treated with 45 mg/kg of tofacitinib. AIA rats treated with 15 mg/kg tofacitinib had significantly ($p<0.05$) reduced ankle inflammation (51% reduction) and bone resorption (67%). At 5 mg/kg, only the decrease in ankle inflammation (35%) was significant. The effect of tofacitinib on summed ankle histopathology scores relative to the vehicle control AIA rats was dose dependent across the entire range of doses tested, and significant ($p<0.05$) at doses of 5 (33% reduction), 15 (52% reduction) and 45 mg/kg (72% reduction) of tofacitinib.

CIA – Figure 5C is a representative ankle diameter vs time plot for diseased animals treated with tofacitinib (vehicle, 0.5, 1.5, 5, 15, and 45 mg/kg PO) on days 1 to 7 of established disease. Daily ankle diameter measurements were significantly ($p<0.05$) reduced toward normal for CIA rats given 0.5 mg/kg (days 6 to 8), 1.5 mg/kg (days 2 to 8), 5 mg/kg (days 2 to 8), 15 mg/kg (days 2 to 8), and 45 mg/kg (days 2 to 8) of tofacitinib when compared to vehicle control rats. AUC_{ankle} was significantly ($p<0.05$) and dose responsively reduced toward normal for CIA rats treated with 1.5 mg/kg (42% reduction), 5 mg/kg (77% reduction), 15 mg/kg (92% reduction), and 45 mg/kg (95% reduction) tofacitinib when compared to vehicle controls. Tofacitinib treatment resulted in a dose dependent decrease in ankle histopathology scores in CIA rats (see Figure 5D). All individual ankle histopathology parameters (inflammation, pannus, cartilage damage, bone resorption) were significantly ($p<0.05$) reduced relative to the vehicle controls for CIA rats treated with 5, 15, and 45 mg/kg of tofacitinib. CIA rats treated with 1.5 mg/kg tofacitinib had significantly ($p<0.05$) reduced ankle pannus (49% reduction), and bone resorption (49% reduction). Accordingly, the effect of tofacitinib on summed ankle histopathology scores relative to the vehicle control CIA rats was dose dependent and significant ($p<0.05$) at doses of 1.5 (40% reduction), 5 (77% reduction), 15 (94% reduction) and 45 mg/kg (100% reduction) of tofacitinib. Effects of tofacitinib were more pronounced at similar doses in CIA rats when compared to AIA rats (Figure 5).

Dexamethasone: *AIA* – Figure 6A is a representative ankle diameter vs time plot for diseased animals treated with dexamethasone (vehicle, 0.0125, 0.025, 0.05, 0.1, and 0.2 mg/kg PO) on days 1 to 7 of established disease. Daily ankle diameter measurements were significantly ($p<0.05$) reduced toward normal for AIA rats given 0.0125 mg/kg (day 4), 0.025 mg/kg (days 3 to 8), 0.05 mg/kg (days 2 to 8), 0.1 mg/kg (days 2 to 8), and 0.2 mg/kg (days 2 to 8) of dexamethasone when

compared to vehicle control rats. AUC_{ankle} was significantly (p<0.05) and dose responsively reduced toward normal for AIA rats treated with 0.025 mg/kg (27% reduction), 0.05 mg/kg (39% reduction), 0.1 mg/kg (58% reduction), and 0.2 mg/kg (82% reduction) dexamethasone when compared to vehicle controls. Dexamethasone treatment resulted in a dose dependent decrease in ankle histopathology scores in AIA rats (see Figure 6B). All individual ankle histopathology parameters (inflammation, pannus, cartilage damage, bone resorption) were significantly (p<0.05) reduced relative to the vehicle control for AIA rats treated with 0.05, 0.1, and 0.2 mg/kg of dexamethasone. AIA rats treated with 0.025 mg/kg dexamethasone had significantly (p<0.05) reduced ankle inflammation (23% reduction), and bone resorption (42% reduction). The effect of dexamethasone on summed ankle histopathology scores relative to the vehicle control AIA rats was dose dependent across the entire range of doses tested, and significant (p<0.05) at doses of 0.025 (30% reduction), 0.05 (52% reduction), 0.1 (62% reduction), and 0.2 mg/kg (83% reduction) of dexamethasone.

CIA – Figure 6C is a representative ankle diameter vs time plot for diseased animals treated with dexamethasone (vehicle, 0.0125, 0.025, 0.05, 0.1, and 0.2 mg/kg PO) on days 1 to 7 of established disease. Daily ankle diameter measurements were significantly (p<0.05) reduced toward normal for CIA rats given 0.0125 mg/kg (day 3), 0.025 mg/kg (days 2 to 8), 0.05 mg/kg (days 2 to 8), 0.1 mg/kg (days 2 to 8), and 0.2 mg/kg (days 2 to 8) of dexamethasone when compared to vehicle control rats. AUC_{ankle} was significantly (p<0.05) and dose responsively reduced toward normal for CIA rats treated with 0.025 mg/kg (82% reduction), 0.05 mg/kg (92% reduction), 0.1 mg/kg (96% reduction), and 0.2 mg/kg (98% reduction) dexamethasone when compared to vehicle controls. Dexamethasone treatment resulted in a dose dependent decrease in ankle histopathology scores in CIA rats (see Figure 6D). All individual ankle histopathology

parameters (inflammation, pannus, cartilage damage, bone resorption) were significantly ($p<0.05$) reduced relative to the vehicle controls for CIA rats treated with 0.025, 0.05, 0.1, and 0.2 mg/kg of dexamethasone.   Accordingly, the effect of dexamethasone on summed ankle histopathology scores relative to the vehicle control CIA rats was dose dependent and significant ($p<0.05$) at doses of 0.025 (75% reduction), 0.05 (90% reduction), 0.1 (99% reduction) and 0.2 mg/kg (99% reduction) of dexamethasone.   Effects of dexamethasone were more pronounced at similar doses in CIA rats when compared to AIA rats (Figure 6).

Anti-inflammatory Activity on Ankle Swelling

Characterization of anti-inflammatory activity on ankle swelling in AIA and CIA rats of systemic concentrations of indomethacin, methotrexate, etanercept and tofacitinib was determined through a PK-PD modeling approach. Dexamethasone AIA and CIA studies were not included in this analysis as corticosteroids are typically administered as acute local injections making relationships between systemic concentrations and drug effect less clinically relevant. A PK-PD model (Figure 1A) characterizing systemic drug effect (see Methods for details) was used to fit ankle diameter data from preclinical studies. The indirect response PK-PD model described in Figure 1A (equation) assumes that drug acts to reduce ankle swelling through increasing the rate constant, I_{AS}. The choice of using an anti-arthritis effect that was described by a saturable equation (Equation 2) versus a linear equation (Equation 3) was based on model fitting statistics (see Methods). Inflammation and subsequent ankle swelling appeared to have a faster onset rate in AIA rats and is reflected in k_{in} estimates that were approximately two-fold higher in AIA compared to CIA rats in all studies (Supplemental Table 3). There was good concordance between the predicted ankle diameter obtained from the PK-PD fits and observed

ankle diameters indicating that the PK-PD models used adequately characterize drug effects on

ankle inflammation in AIA (Figure 7C) and CIA rats (Figure 7D).

Direct comparisons of pharmacodynamic parameters reflective of anti-inflammatory activity

on ankle swelling could not be made across all anti-arthritis agents tested since the PK-PD models

used to characterize each agent were often not identical (see Supplemental Table 3). However,

comparisons of anti-inflammatory activity relative to clinically relevant exposures could be

accomplished through simulations using the preclinical PK-PD models and clinical

pharmacokinetics, dose, and regimen (see Figure 1B). Figure 7A and 7B show a representative CIA

ankle diameter-time profile and an associated PK-PD model ankle diameter simulation using a

clinical regimen for indomethacin. Table 2 summarizes the percent inhibition of ankle diameter

AUC (AUC_{ankle}) following clinical regimen simulations for indomethacin, methotrexate, etanercept

and tofacitinib. None of the agents tested inhibited AUC_{ankle} completely. Indomethacin and

tofacitinib appear to be the most active agents in both preclinical models with maximum inhibition

of AUC_{ankle} being 52 % and 63% in CIA rats, respectively. Inhibition of AUC_{ankle} by indomethacin

and tofacitinib inhibition was less in AIA rats, 40% and 27%, respectively. The diminished anti-

inflammatory activity in AIA rats appears to be a consequence of more aggressive inflammation in

AIA rats as evident by an approximately 2-fold higher k_{in} in AIA compared to CIA rats mentioned

above. Inhibition of AUC_{ankle} by methotrexate and etanercept at clinically relevant exposures was

less effective compared to indomethacin and tofacitinib being $\leq 16\%$ in AIA and CIA rats.

Ankle Histopathology at Clinically Relevant Exposures

Characterization of relationships between ankle histopatholgy summed scores (AHSS) and systemic

drug concentrations of indomethacin, etanercept and tofacitinib was performed either using either a

standard E_{max} equation (Equation 6) or an E_{max} equation with a linear effect component (Equation

7). Dexamethasone AIA and CIA studies were not included in this analysis as corticosteroids are

typically administered as acute local injections making relationships between systemic

concentrations and drug effect less clinically relevant. Figure 8 shows plots of percent inhibition of

end of study ankle histopathology summed scores versus steady-state drug concentrations and the

associated model fitted lines and pharmacodynamics parameters. Of note, the estimated E_{max} of

tofacitinib in CIA (Figure 8F) exceeded 100% (i.e.105%) which is not possible by definition. As

this value was an estimation, and was very close to the theoretical E_{max} maximum of 100%, we

chose to report the value as the fitted estimated value. Methotrexate histopatholgy summed scores

were not modeled due to inadequate dose responsiveness characterization for modeling purposes

(see Figure 3B and 3D).

Estimated pharmacodynamics parameters were used to calculate the % inhibition of AHSS

at clinical steady-state concentrations and results are presented in Table 2. For methotrexate,

percent inhibition of ankle histopathology was approximated by comparing clinical steady state

concentrations to those estimated for each dose level based on measure pharmacokinetics from

satellite group. The estimated steady-state concentration at 0.3 mg/kg dose level in both AIA

(0.0117 µM) and CIA (0.00832 µM) rats was similar to that estimated in patients (0.0133 µM).

Therefore, the percent inhibition of ankle histopathology summed scores at clinically relevant

exposures was approximated to values observed at the 0.3 mg/kg dose in AIA (~8%) and CIA

(~5%) rats. Similar to the analysis of anti-inflammatory activity associated with ankle swelling, no

anti-arthritis agent tested caused complete inhibition of ankle histology at clinically relevant steady-

state concentrations. Once again, indomethacin and tofacitinib were the most effective in inhibiting

ankle histopathology in CIA rats resulting in 45% and 56% inhibition of ankle histopathology,

respectively. Both drugs caused less inhibition of ankle histopathology in AIA compared to CIA

rats which is likely due AIA rats exhibiting more aggressive disease. Similar to indomethacin and

tofacitinib, etanercept exhibited more activity on ankle histopathology assessments in CIA rats but

to a lesser magnitude. Methotrexate was the least active on ankle histopathology of all agents

tested.

DISCUSSION

Despite their wide use and their acknowledged importance to drug development, the ability of rodent immune-mediated arthritis models to quantitatively predict therapeutic activity of anti-arthritis agents is poorly understood. The clinical relevance of rodent immune-mediated arthritis models have been investigated and reviewed by others (Bendele et al., 1999; Kannan et al., 2005; Hegen et al., 2008). However, reported investigations provide qualitative or, at best, semi-quantitative comparisons of preclinical and clinical efficacy as known species differences in pharmacokinetics of anti-arthritis agents were not accounted for. In a recent manuscript reviewing the use of translational PK-PD analysis in pharmaceutical industry, a shortage of quantitative clinical validation of translatable-preclinical models was reported for autoimmune diseases including RA (Wong et al., 2017). The current work provides a detailed quantitative examination of drug exposure-effect relations in rat AIA and CIA using PK-PD analysis in order to evaluate preclinical efficacy in context of clinically relevant drug exposures. Therapeutic efficacy rather than prophylactic efficacy in AIA and CIA rats was evaluated since therapeutic efficacy has been found to be more predictive of clinical efficacy in human RA patients (Hegen et al., 2008).

The four anti-rheumatic agents that were used in our evaluation include indomethacin, methotrexate, etanercept (an anti-TNF biologic), and tofacitinib (a recently approved oral JAK inhibitor). Unlike the other drug evaluated, indomethacin is used to manage symptoms of RA such as pain, stiffness, inflammation, and joint swelling at clinically relevant doses (Saul and Korlipara, 1991; Burke et al., 2006; Combe et al., 2017). Indomethacin is not considered to be a "disease modifying" anti-rheumatic drug and therefore is not expected to stop the progression of disease and prevent joint destruction. In contrast, methotrexate (conventional synthetic DMARD), etanercept

(biologic DMARD), and tofacitinib (targeted synthetic DMARD) represent different classes of

DMARDS that are used clinically to prevent or reduce the risk of RA associated joint damage

(Chatzidionysiou et al., 2017; Combe et al., 2017; Ramiro et al., 2017). Finally, dexamethasone (a

corticosteroid) typically delivered by local injection to RA patients was included as a common

positive control in both preclinical models.

The efficacy endpoints used in our analysis were inhibition of AUC_{ankle} and inhibition of

AHSS. Increases in ankle diameter (assessed as increases in AUC_{ankle}) in AIA and CIA rats

result from edema of the joint and serves as a measure of inflammation. The AHSS comprised

of individual histopathology scores (i.e. inflammation, pannus, cartilage damage and bone

resorption) serves as a measurement of underlying structural changes to the bone caused by

disease progression. For each drug tested, inhibition of both AUC_{ankle} and AHSS scores were

generally comparable in both magnitude and rank order (Tables 2). Of interest, methotrexate

showed the lowest magnitude of effect on AHSS at clinically relevant drug concentrations

despite being the standard of care DMARD for the clinical treatment of RA (Combe et al., 2017).

Overall, based on both the AUC_{ankle} and the AHSS inhibition data, the rank ordering of

preclinical activity was tofacitinib > etanercept ≥ methotrexate.

Direct comparisons with clinical activity in RA are difficult as assessment of clinical

anti-rheumatic activity is only pseudo-quantitative in nature. However, emerging clinical data is

consistent with our rank ordering of drug activity.   Tofacitinib monotherapy appears to be more

effective than methotrexate in methotrexate naïve RA patients (patients who have not previously

received methotrexate or therapeutic doses of methotrexate) in the reduction of RA signs and

symptoms and inhibiting the progression of structural joint damage (Lee et al., 2014; Strand et

al., 2016). Comparisons of the clinical efficacy of etanercept and methotrexate monotherapy

were not as clear-cut. A meta-analysis of clinical efficacy data of four anti-TNF biologics

including etanercept given as monotherapy compared to methotrexate monotherapy showed that

while risk ratios (an efficacy metric) favored the anti-TNF biologics, they do not reach statistical

significance (Aaltonen et al, 2012). Similarly, differences between etanercept and methotrexate

activity on AHSS were not entirely consistent with both compounds showing similar efficacy in

AIA rats, but etanercept having greater efficacy in CIA rats (Table 2).

As a note of caution, despite the apparent concordance of our preclinical efficacy data for

DMARDs to clinical efficacy, the predictive value of preclinical efficacy in AIA and CIA rats is

not without flaw. Of note, indomethacin showed equal or often better efficacy than other

DMARDs on inhibiting structural joint damage in AIA and CIA rats (as assessed by inhibition of

AHSS) despite having limited ability to prevent joint damage clinically in RA patients. The

comparable efficacy of indomethacin on both AUC_{ankle} and the AHSS serves as a clear example

of an inability of AIA and CIA rats to provide differentiation between treatment of disease

symptoms (joint inflammation) and disease progression (joint damage) that is observed

clinically. Despite this, applications of translational PK-PD modeling of preclinical efficacy in

AIA and CIA rats does have value in drug development. The translational value of PK-PD

analyses can be grouped into two broad categories; 1) rank ordering of new anti-arthritis

therapies in context of relevant clinical concentrations and 2) characterization of quantitative

relationships of biological pathways important to RA.

Rank ordering of new anti-arthritis therapies in context of relevant clinical concentrations

A central theme of our work described in the current manuscript is the ability of PK-PD analysis

to normalize species difference in pharmacokinetics in order to properly context preclinical

31

activity to clinically relevant drug concentrations in humans. In theory, this would allow a fair

comparison of efficacy of new therapies to existing drugs on the market. The current study

suggests that the clinical activity of anti-rheumatic drugs can be rank ordered based on

preclinical activity despite the confounding results with indomethacin. Ideally, rank ordering of

compound efficacy is best performed with the following two considerations. First, the

appropriate choice of model is important for meaningfully ranking compounds. Since RA is a

heterogeneous disease and is likely manifested by different pathological pathways, RA patients

show varying responses to any particular drug therapy that normally interferes one or few

biological pathways. Thus, the preclinical evaluation of a novel compound's efficacy should be

performed in models sharing the appropriate pathological pathways in human RA. Animal

model selection in such a manner would provide a biologically plausible rational for improved

efficacy when comparing new drug candidates to either marketed drugs or more advanced

compounds targeting the same biological pathway. Second, testing in more than one model is

preferred whenever possible to evaluate the contribution of different genetic backgrounds and

inflammatory conditions. An example of a rank ordering approach is described in a case study

from recent manuscript from pharmaceutical industry where preclinical PK-PD analysis of

efficacy data in AIA rats was used to rank order and select second-generation drug candidates

with anticipated improved efficacy compared to an advanced competitor compound sharing the

same mechanism of action (Wong et al., 2017). As a final note, rank ordering of efficacy is

likely more reliable when comparing drugs/compounds that share the same biological target.

Further, preclinical models of arthritis differ from human RA in that these models have a more

aggressive form of the disease and contributions from various biological drivers of preclinical

disease may differ from human RA. For example, the inflammatory stimuli or pathways, which

triggered leukocyte influx, joint swelling, and bone damage, in these models may differ from those in human RA. Thus, the quantitative assessment of preclinical efficacy endpoints may only be useful for the rank ordering of those relevant pathways in the selected models. For instance, our PK-PD modeling results with methotrexate and etanercept show that at clinically relevant concentrations the preclinical activity in therapeutic AIA and CIA rats is rather low for these two clinically effective DMARDs (Tables 2), suggesting the pathogenic contributions of TNF-α pathway in these models may not be as high as those in human RA.

Characterization of quantitative relationships of biological pathways important to RA

A second aspect of the translational value of PK-PD analysis of preclinical arthritis models involves the quantitative characterization of biological pathways central to the disease through the development of mechanistic PK-PD models. These mechanistic PK-PD models offer a means to evaluate a). the degree of importance of biological pathway to an immune mediated disease in an *in vivo* setting, b) assessment of *in vitro* to *in vivo* correlation of drug potency, c) exploration of new biomarkers that quantitatively assess their modulation with an efficacy outcome, and d) assessment of synergism following inhibition of more than one biological pathway. Some of these applications have been reported and used in pharmaceutical industry (Wong et al., 2017). Finally, the resultant mechanistic PK-PD models can be used to influence design of early clinical trials including setting of pharmacodynamic biomarker endpoints, generating therapeutic and toxicity indexes, and providing insights into therapeutic mechanisms related to efficacy.

In summary, the current work describes a comprehensive effort to provide clinical validation of therapeutic AIA and CIA in rats using translational PK-PD analysis. Based on our work, PK-PD analysis of preclinical efficacy data can be used to rank order the clinical efficacy of new therapies for RA. In addition, we propose that PK-PD modeling of preclinical efficacy data improves the quantitative understanding of biological pathways involved in RA and can provide value in the search for new and novel therapies. Finally, the described approach to clinically validate therapeutic AIA and CIA in rats can be applied to other animal models of autoimmune disease.

ACKNOWLEDGMENTS

AUTHORSHIP CONTRIBUTIONS

Participated in research design: Wong, Hop

Conducted experiments: Deng

Contributed new reagents or analytical tools: Deng

Performed data analysis: Wong, Liu, Ouyang, Wright; Hop

Wrote or contributed to writing of manuscript: Wong, Liu, Ouyang, Deng Wright, Hop

REFERENCES

Aaltonen KJ, Virkki LM, Malmivaara A, Konttinen YT, Nordstrom DC, and Blom M. (2012) Systematic Review and Meta-Analysis of the Efficacy and Safety of Existing TNF Blocking Agents in Treatment of Rheumatoid Arthritis *PLoS ONE* 7: e30275.

Arrowsmith J and Miller P. (2013) Trial watch: phase II and phase III attrition rates 2011-2012. *Nat Rev Drug Discov*. **12**:569. doi: 10.1038/nrd4090.

Bendele A (2001) Animal models of rheumatoid arthritis. *J Musculoskelet Neuronal Interact* **1:** 377-385.

Bendele A, McComb J, Gould T, McAbee T, Sennello G, Chlipala E and Guy M. (1999) Animal models of arthritis: relevance to human disease. *Toxicol Pathol*. 27:134-142.

Burke A, Smyth E, Fitzgerald GA. (2006) Analgesic-antipyretic agents, pharmacotherapy of gout. In: Brunton, L.L., Lazo, J.S. and Parker, K.L. (Eds.), Goodman and Gilman. Pharmacological Bases of Therapeutics. 11th edition, McGraw Hill Company Incorporation, New York; 671-715

Bolon B, Stolina M, King C, Middleton S, Gasser J, Zack D, and Feige U. (2011) Rodent preclinical models for developing novel antiarthritic molecules: comparative biology and preferred methods for evaluating efficacy. *J Biomed Biotechnol*. 2011:569068.

Caplazi P, Baca M, Barck K, Carano RA, DeVoss J, Lee WP, Bolon B and Diehl L. (2015) Mouse Models of Rheumatoid Arthritis. *Vet Pathol*. pii: 0300985815588612.

Chatzidionysiou K, Emamikia S, Nam J, Ramiro S, Smolen J, van der Heijde D, Dougados M, Bijlsma J, Burmester G, Scholte M, and van Vollenhoven R, Landewé R (2017) Efficacy of glucocorticoids, conventional and targeted synthetic disease-modifying antirheumatic drugs: a systematic literature review informing the 2016 update of the EULAR recommendations for the management of rheumatoid arthritis. *Ann Rheum Dis*. 76:1102-1107.

Cohen S, Zwillich SH, Chow V, Labadie RR and Wilkinson B (2010) Co-administration of the JAK inhibitor CP-690,550 and methotrexate is well tolerated in patients with rheumatoid arthritis without need for dose adjustment. *Br J Clin Pharmacol*. 69:143-151.

Combe B, Landewe R, Daien CI, Hua C, Aletaha D, Álvaro-Gracia JM, Bakkers M, Brodin N, Burmester GR, Codreanu C, Conway R, Dougados M, Emery P, Ferraccioli G, Fonseca J, Raza K, Silva-Fernández L, Smolen JS, Skingle D, Szekanecz Z, Kvien TK, van der Helm-van Mil A, van Vollenhoven R. (2017) 2016 update of the EULAR recommendations for the management of early arthritis. *Ann Rheum Dis*. **76**:948-959.

Gilbaldi M and Perrier D. (1982) *Pharmacokinetics 2nd Edition* , Marcel Dekker, New York.

Godfrey C, Sweeney K, Miller K, Hamilton R, and Kremer J (1998) The population
pharmacokinetics of long-term methotrexate in rheumatoid arthritis. *Br J Clin Pharmacol*.
46:369-376

Hegen M, Keith JC Jr, Collins M, and Nickerson-Nutter CL. (2008) Utility of animal models for
identification of potential therapeutics for rheumatoid arthritis. *Ann Rheum Dis*. **67**:1505-1515.

Helleberg L. (1981) Clinical Pharmacokinetics of indomethacin. *Clin Pharmacokinet*. **6**:245-258.

Kannan K, Ortmann RA, and Kimpel D. (2005) Animal models of rheumatoid arthritis and their
relevance to human disease. *Pathophysiology*. 12:167-181.

Keystone EC, Schiff MH, Kremer JM, Kafka S, Lovy M, DeVries T and Burge DJ (2004) Once-
weekly administration of 50 mg etanercept in patients with active rheumatoid arthritis: results of
a multicenter, randomized, double-blind, placebo-controlled trial. *Arthritis Rheum*. 50:353-363.

Kollias G, Papadaki P, Apparailly F, Vervoordeldonk MJ, Holmdahl R, Baumans V, Desaintes
C, Di Santo J, Distler J, Garside P, Hegen M, Huizinga TW, Jüngel A, Klareskog L, McInnes I,
Ragoussis I, Schett G, Hart B', Tak PP, Toes R, van den Berg W, Wurst W and Gay S (2011)
Animal models for arthritis: innovative tools for prevention and treatment. *Ann Rheum Dis*. **70**:
1357-1362

Lee EB, Fleischmann R, Hall S, Wilkinson B, Bradley JD, Gruben D, Koncz T, Krishnaswami S, Wallenstein GV, Zang C, Zwillich SH, van Vollenhoven RF; ORAL Start Investigators. (2014) Tofacitinib versus methotrexate in rheumatoid arthritis. *N Engl J Med*. **370**:2377-2386.

Liu L, Di Paolo J, Barbosa J, Rong H, Reif K and Wong H. (2011) Anti-Arthritis Effect of a Novel Bruton's Tyrosine Kinase Inhibitor in Rat Collagen-Induced Arthritis and Mechanism-Based Pharmacokinetic/Pharmacodynamic Modeling: Relationships between Inhibition of BTK Phosphorylation and Efficacy. J Pharmacol and Exp Ther, 338: 154-163.

Pearson CM. (1956) Development of arthritis, periarthritis and periostitis in rats given adjuvants. *Proc Soc Exp Biol Med*. **91**: 95-101.

Ramiro S, Sepriano A, Chatzidionysiou K, Nam JL, Smolen JS, van der Heijde D, Dougados M, van Vollenhoven R, Bijlsma JW, Burmester GR, Scholte-Voshaar M, Falzon L, and Landewé RBM. (2017) Safety of synthetic and biological DMARDs: a systematic literature review informing the 2016 update of the EULAR recommendations for management of rheumatoid arthritis. Ann Rheum Dis. **76**:1101-1136.

Saul PA and Korlipara K (1991) Acemetacin and indomethacin in the treatment of rheumatoid arthritis: a double-blind comparative study in general practice. *Curr Med Res Opin*. 12:332-341.

Schuck E, Bohnert T, Chakravarty A, Damian-Iordache V, Gibson C, Hsu CP, Heimbach T, Krishnatry AS, Liederer BM, Lin J, Maurer T, Mettetal JT, Mudra DR, Nijsen MJ, Raybon J,

Schroeder P, Schuck V, Suryawanshi S, Su Y, Trapa P, Tsai A, Vakilynejad M, Wang S, and Wong H. (2015) Preclinical pharmacokinetic/pharmacodynamic modeling and simulation in the pharmaceutical industry: an IQ consortium survey examining the current landscape. *AAPS J.* **17**:462-473.

Spilker ME, Chen X, Visswanathan R, Vage C, Yamazaki S, Li G, Lucas J, Bradshaw-Pierce EL, and Vicini P. (2017) Found in Translation: Maximizing the Clinical Relevance of Nonclinical Oncology Studies. *Clin Cancer Res*. **23**:1080-1090.

Strand V, Lee EB, Fleischmann R, Alten RE, Koncz T, Zwillich SH, Gruben D, Wilkinson B, Krishnaswami S, and Wallenstein G (2016) Tofacitinib versus methotrexate in rheumatoid arthritis: patient-reported outcomes from the randomised phase III ORAL Start trial. *RMD Open*. 2:e000308

Trentham DE, Townes AS, and Kang AH (1977) Autoimmunity to type II collagen: an experimental model of arthritis. *J Exp Med* **146:** 857-868.

Wong H, Choo EF, Alicke B, Ding X, La H, McNamara E, Theil FP, Tibbitts J, Friedman LS, Hop CECA, Gould SE. (2012a) Anti-tumor activity of targeted and cytotoxic agents in murine subcutaneous tumor models correlates with clinical response *Clin Cancer Res*. **18**: 3846-3855.

41

Wong H, Vernillet L, Peterson A, Ware JA, Lee L, Martini J-F, Yu P, Li C, Del Rosario G, Choo EF, Hoeflich KP, Shi Y, Aftab BT, Aoyama R, Lam ST, Belvin M, Prescott J. (2012b) Bridging the Gap between Preclinical and Clinical Studies Using PK-PD Modeling: An Analysis of GDC-0973, a MEK Inhibitor. *Clin Cancer Res*. **18**: 3090-3099.

Wong H and Gould SE. (2016) Translational pharmacokinetic/pharmacodynamic analysis in cancer pharmacology: A tool to maximize the value of antitumor efficacy from tumor bearing mice. Drug Discov Today Technol. **21-22**: 51-56.

Wong H, Bohnert T, Damian-Iordache V, Gibson C, Hsu C-P, Heimbach T, Krishnatry AS, Liederer BM, Lin J, Lu Q, Mettetal JT, Mudra DR, Nijsen MJMA, Schroeder P, Schuck E, Suryawanshi S, Trapa P, Tsai A, Wang H and Wu F. (2017) Translational Pharmacokinetic-Pharmacodynamic Analysis in Pharmaceutical Industry: An IQ Consortium PK-PD Discussion Group Perspective. *Drug Discov Today*. **22**:1447-1459. doi: 10.1016/j.drudis.2017.04.015.

42

FOOTNOTES

Send reprint requests to: Dr. Harvey Wong, The University of British Columbia, 2405 Wesbrook

Mall, Vancouver, BC, Canada. V6T 1Z3. E-mail: harvey.wong@ubc.ca.

LEGENDS FOR FIGURES

Figure 1 The PK-PD modeling and simulation process used to translate preclinical ankle joint swelling measurements is depicted. Ankle joint swelling in AIA or CIA rats was described using a standard indirect response model (A). AD (inches) is defined as the ankle diamater, k_{in} (inches×day^{-1}) is the rate of increase in ankle diameter, and I_{AS} (day^{-1}) is the rate constant describing the anti-ankle joint swelling effect of the agents used in the AIA and CIA studies. The simulation process integrating human pharmacokinetics is described in B. Pharmacodynamic parameters relating drug concentration to anti-ankle joint swelling effect are estimated for each drug tested in AIA and CIA rats following fitting of the indirect response model to ankle diameter measurements using rat pharmacokinetics. Simulations of clinical regimen were carried out using the pre-clinical PK-PD model, the estimated pharmacodynamics parameters from preclinical AIA or CIA studies and human pharmacokinetics from the literature (see Supplemental Table 1)

Figure 2 Ankle diameter vs time profile in AIA (2A) and CIA (2C) rats given 0.1, 0.3, 1, 3 or 6 mg/kg indomethacin PO daily on days 1 to 7 of established disease. Corresponding end of study ankle histopathology scores in AIA (2B) and CIA (2D) rats following indomethacin treatment. Each histology parameter (inflammation, pannus, cartilage damage, and bone resorption) is scored from 0 to 7 for AIA rats and 0 to 5 for CIA rats, and is represented by patterned bars indicated by the figure legend. Total height of each bar represents the mean summed ankle histopathology score for the specific

dose group that can have a maximum value of 28 for AIA rats and 20 for CIA rats.

Error bars in plots represent standard error of the mean.

Figure 3 Ankle diameter vs time profile in AIA (3A) and CIA (3C) rats given 0.1, 0.3, 1, 3 or

10 mg/kg methotrexate PO daily on days 1 to 7 of established disease. Corresponding

end of study ankle histopathology scores in AIA (3B) and CIA (3D) rats following

methotrexate treatment. Each histology parameter (inflammation, pannus, cartilage

damage, and bone resorption) is scored from 0 to 7 for AIA rats and 0 to 5 for CIA

rats, and is represented by patterned bars indicated by the figure legend. Total height

of each bar represents the mean summed ankle histopathology score for the specific

dose group that can have a maximum value of 28 for AIA rats and 20 for CIA rats.

Error bars in plots represent standard error of the mean

Figure 4 Ankle diameter vs time profile in AIA (4A) and CIA (4C) rats given 0.3, 1, 3, 10 or 30

mg/kg etanercept via subcutaneous injection every third day on days 1, 4, and 7 of

established disease. Corresponding end of study ankle histopathology scores in AIA

(4B) and CIA (4D) rats following etanercept treatment. Each histology parameter

(inflammation, pannus, cartilage damage, and bone resorption) is scored from 0 to 7

for AIA rats and 0 to 5 for CIA rats, and is represented by patterned bars indicated by

the figure legend. Total height of each bar represents the mean summed ankle

histopathology score for the specific dose group that can have a maximum value of 28

for AIA rats and 20 for CIA rats. Error bars in plots represent standard error of the

mean

Figure 5 Ankle diameter vs time profile in AIA (5A) and CIA (5C) rats given 0.5, 1.5, 5, 15 or 45 mg/kg tofacitinib PO daily on days 1 to 7 of established disease. Corresponding end of study ankle histopathology scores in AIA (5B) and CIA (5D) rats following tofacitinib treatment. Each histology parameter (inflammation, pannus, cartilage damage, and bone resorption) is scored from 0 to 7 for AIA rats and 0 to 5 for CIA rats, and is represented by patterned bars indicated by the figure legend. Total height of each bar represents the mean summed ankle histopathology score for the specific dose group that can have a maximum value of 28 for AIA rats and 20 for CIA rats. Error bars in plots represent standard error of the mean

Figure 6. Ankle diameter vs time profile in AIA (6A) and CIA (6C) rats given 0.0125, 0.025, 0.05, 0.1 or 0.2 mg/kg dexamethasone PO daily on days 1 to 7 of established disease. Corresponding end of study ankle histopathology scores in AIA (6B) and CIA (6D) rats following dexamethasone treatment. Each histology parameter (inflammation, pannus, cartilage damage, and bone resorption) is scored from 0 to 7 for AIA rats and 0 to 5 for CIA rats, and is represented by patterned bars indicated by the figure legend. Total height of each bar represents the mean summed ankle histopathology score for the specific dose group that can have a maximum value of 28 for AIA rats and 20 for CIA rats. Error bars in plots represent standard error of the mean

Figure 7. An example of a PK-PD analysis of ankle swelling from a rat arthritis model study is shown. Figure 7A shows a representative plot of mean ankle diameter (AD) versus

46

time for dosing ranging study with indomethacin in rat CIA up to study day 6. Figure

7B shows a representative simulation of clinical regimen of indomethacin using

human pharmacokinetics as described in Figure 1B. Figure 7C shows plots of PK-PD

model predicted mean AD vs. observed AD in AIA rats given indomethacin,

methotrexate, etanercept, and tofacitinib. Figure 7D shows plots of PK-PD model

predicted mean AD vs. observed AD in CIA rats given indomethacin, methotrexate,

etanercept, and tofacitinib. Error bars in plots represent standard error of the mean

Figure 8. Plots of ankle histology summed scores (AHSS) vs steady-state plasma concentrations

(C_{ss}) for indomethacin (A and D), etanercept (B and E), and tofacitinib (C and F). The

squares represent mean observed data. The solid line represents the model predicted

curve.

Table 1. Study Design Information for Anti-Arthritis Agents Tested in AIA and CIA Rats

Drug	Efficacy: Dose and Regimen	Supporting Pharmacokinetics–Doses and Assessment Times
Indomethacin	Vehicle (CMC), 0.1, 0.3, 1, 3 or 6 mg/kg indomethacin was given PO daily on days 1 to 7 of established disease.	0.1, 1, and 6 mg/kg PO indomethacin on day 1 (6 mg/kg) or day 7 (0.1 and 1 mg/kg) of established disease.
Methotrexate	Vehicle (CMC), 0.1, 0.3, or 1 mg/kg methotrexate was given PO daily on days 1 to 7 of established disease.	0.1 and 1 mg/kg PO methotrexate on day 7 of established disease.
Etanercept	Vehicle (sterile water), 0.3, 1, 3, 10 or 30 mg/kg etanercept was given via subcutaneous (SC) injection every third day on days 1, 4, and 7 of established disease.	0.3, 1, 3, 10, and 30 mg/kg SC on day1 and day 7 of established disease.
Tofacitinib	Vehicle (MCT), 0.5, 1.5, 5, 15 or 45 mg/kg tofacitinib was given PO daily on days 1 to 7 of established disease.	0.5, 5, and 45 mg/kg PO tofacitinib on day 7 of established disease.
Dexamethasone	Vehicle (CMC), 0.0125, 0.025, 0.05, 0.1 or 0.2 mg/kg dexamethasone was given PO daily on days 1 to 7 of established disease.	0.0125, 0.05, and 0.2 mg/kg PO dexamethasone on day 7 of established disease.

PO – oral route

SC – subcutaneous route

CMC - 1% carboxymethylcellulose

Table 2. Therapeutic Dose, Percent Inhibition of AUC_{ankle} Following Simulations Using Clinical Regimens, Steady-State Concentration and Corresponding Percent Inhibition of Ankle Histopathology Summed Scores (AHSS).

Drug	Therapeutic Dose	% Inhibition of AUC_{ankle}		C_{ss} ave	% Inhibition AHSS	
		AIA	CIA		AIA	CIA
Indomethacin	25 mg three times daily	40%	52%	1.12 μM[a]	41%	45%
Methotrexate	7.5 mg once weekly	8%	7%	0.0133 μM[b]	~8%	~5%
Etanercept	50 mg once weekly	5%	16%	1.77 μg/mL[c]	14%	29%
Tofacitinib	5 mg twice daily	27%	63%	0.0580 μM[d]	22%	56%

a From Helleberg L, 1981
b Calculated using AUC/τ using data from Godfrey et al., 1998.
c Calculated using AUC/τ using data from Keystone et al., 2004.
d Determined by simulating a 5 mg twice daily dose using data from Cohen et al., 2010.

A. Indirect Response PK-PD Model
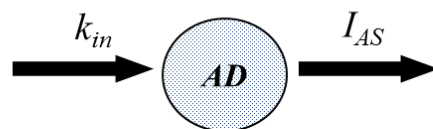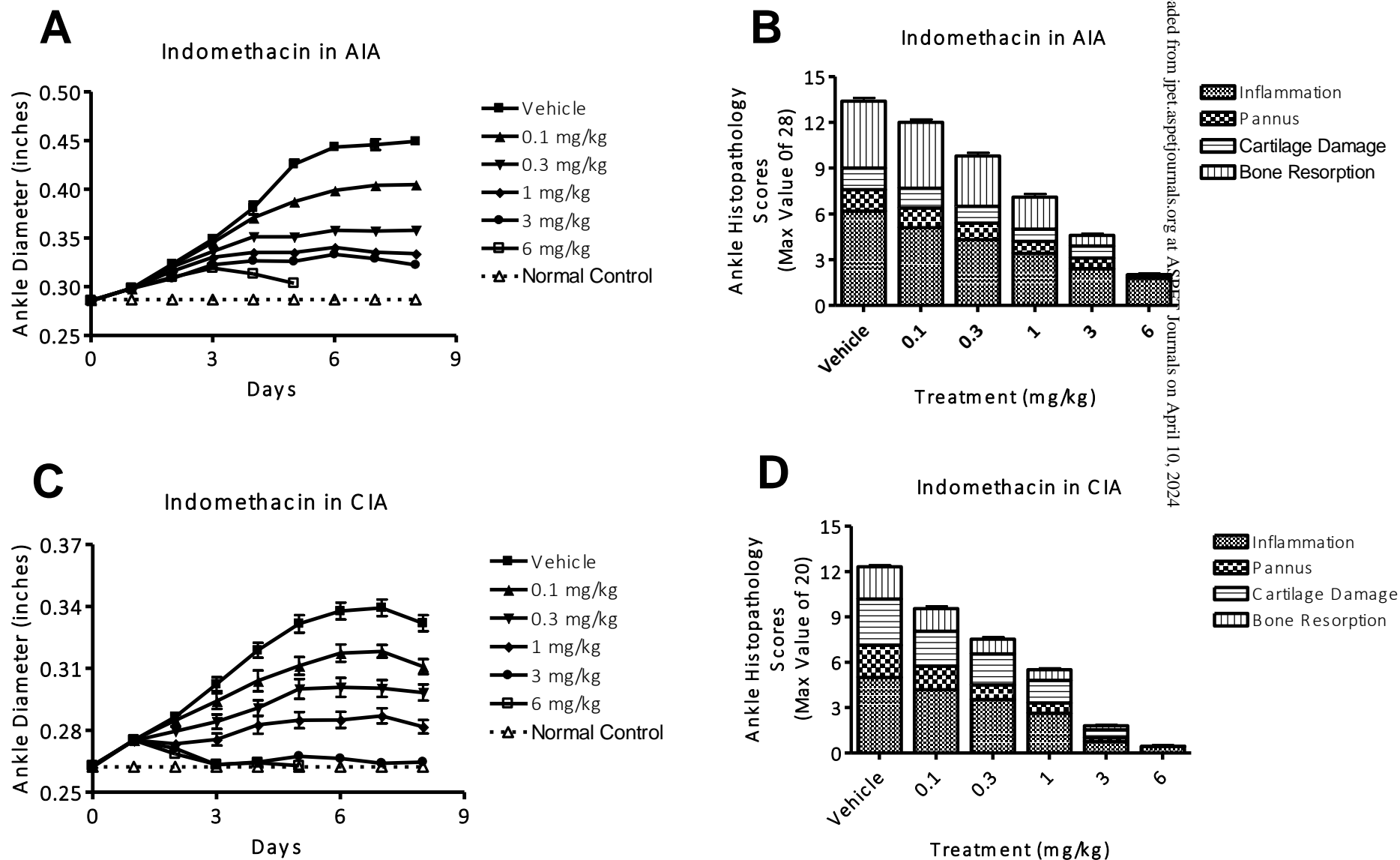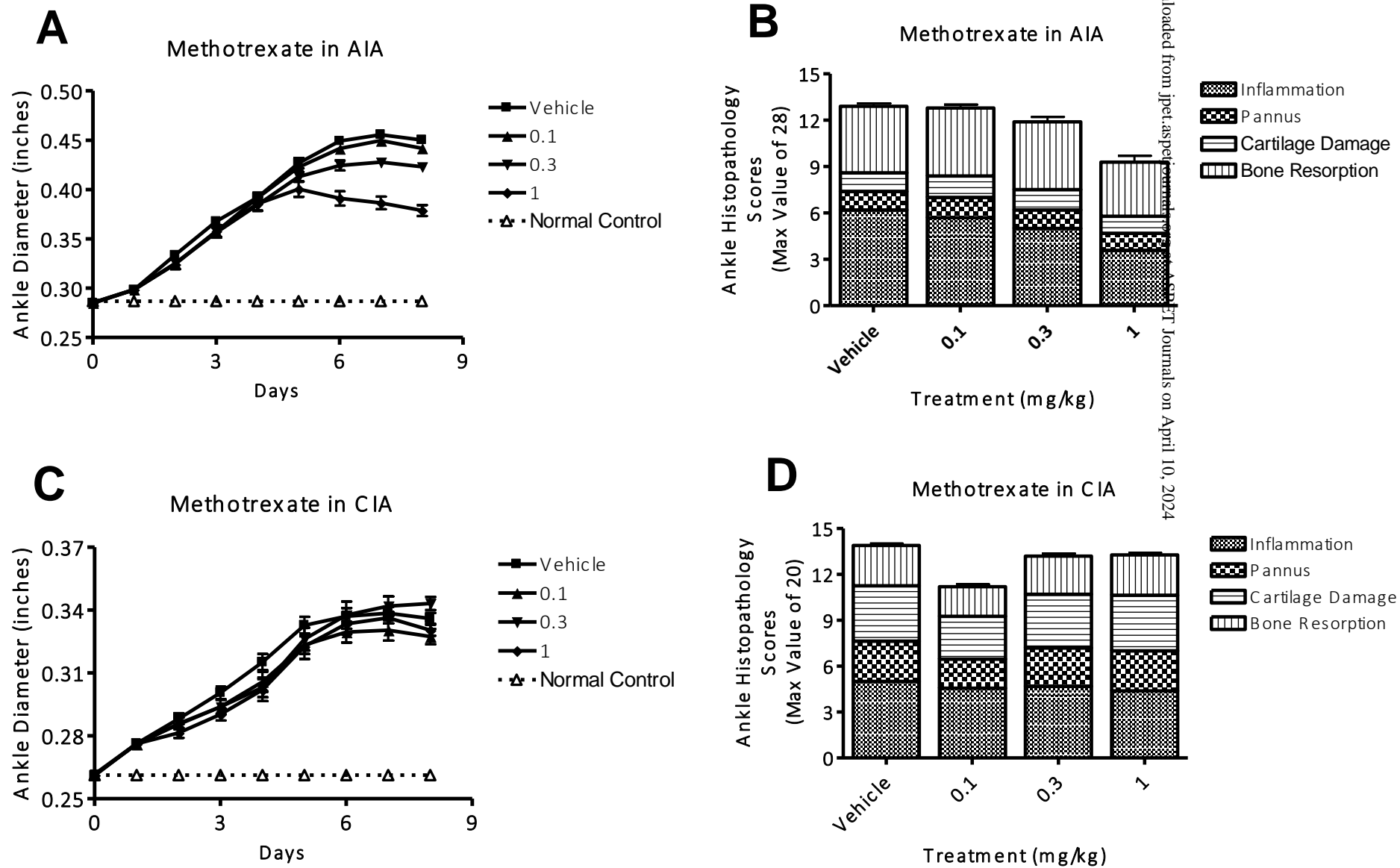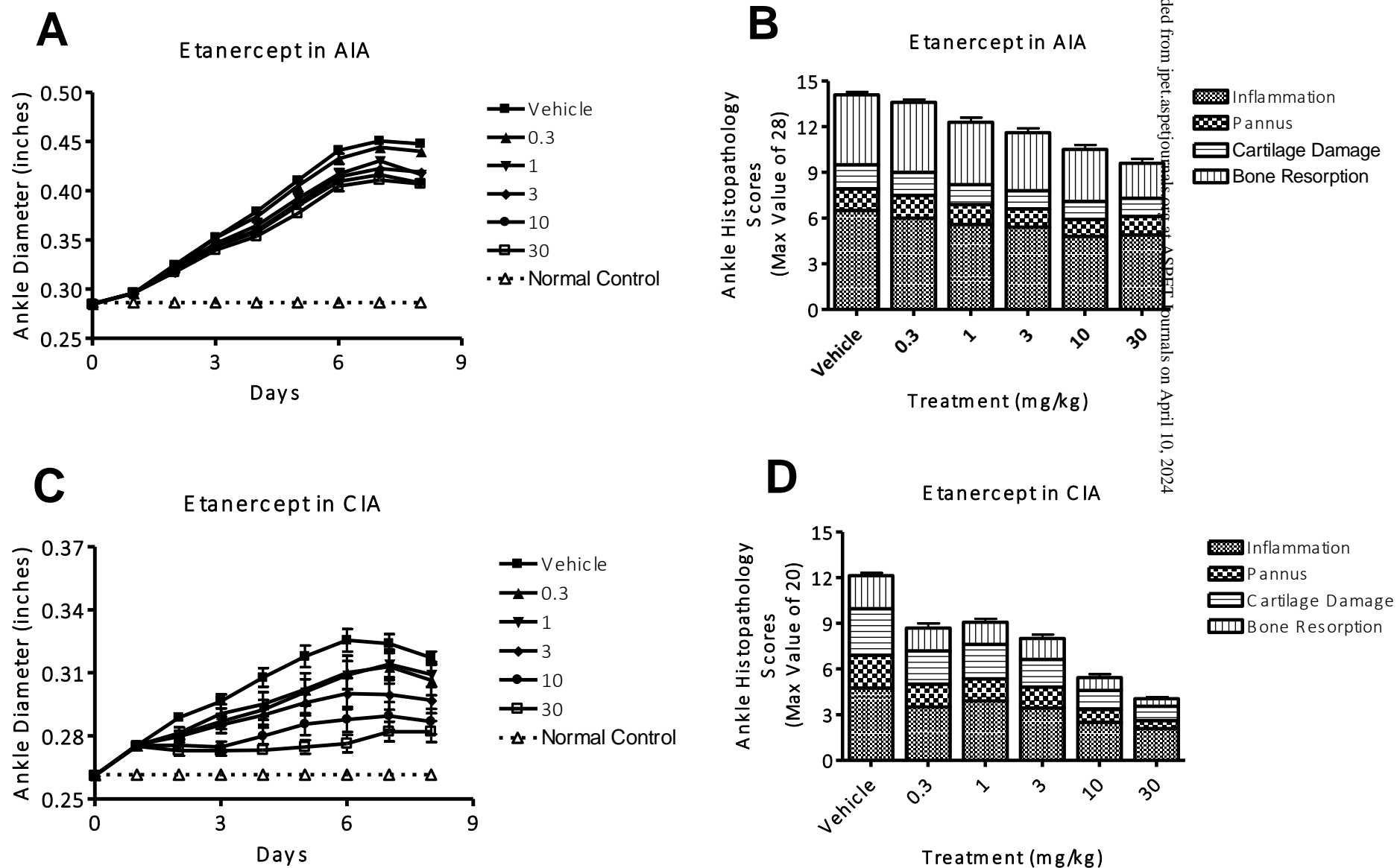

B. Clinical Regimen Simulation
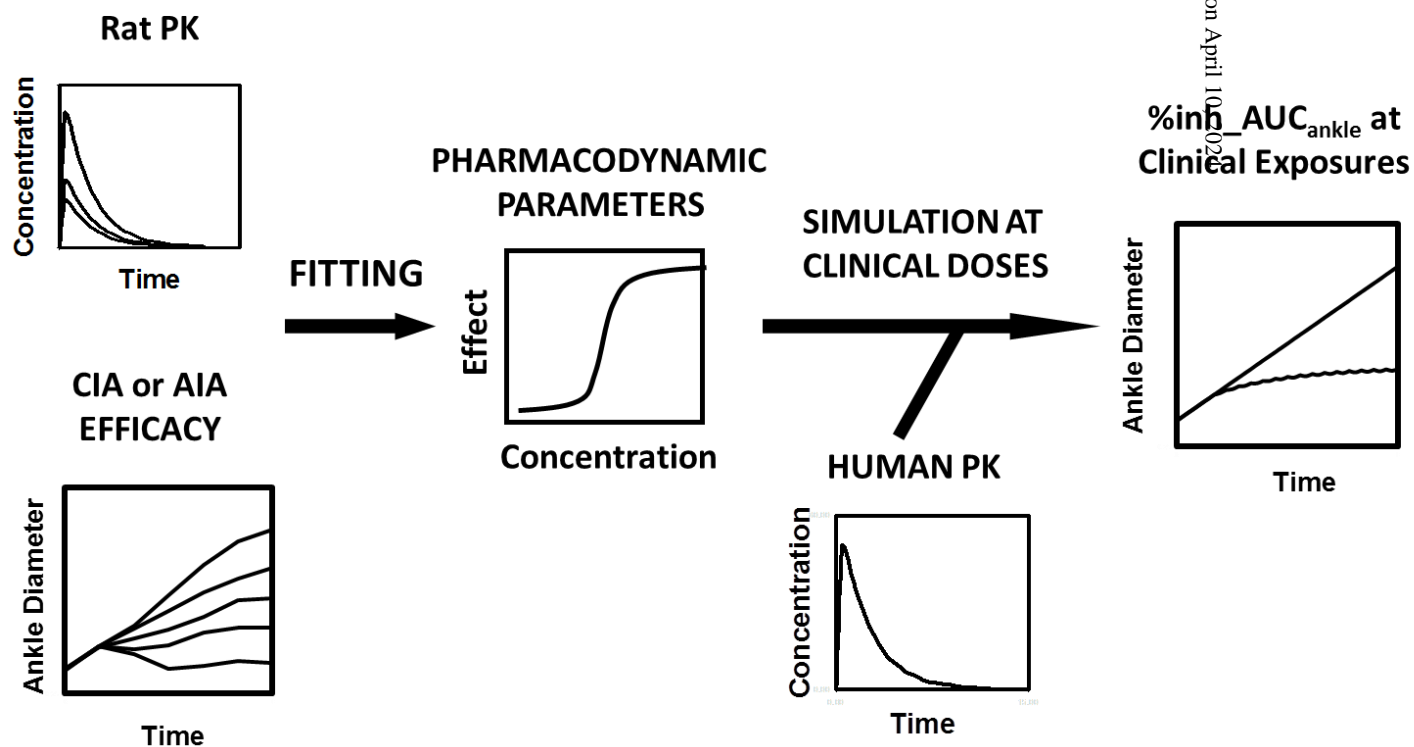
Figure 1

Figure 2

Figure 3

A Etanercept in AIA

B Etanercept in AIA

C Etanercept in CIA

D Etanercept in CIA

Figure 4

A Tofacitinib in AIA

B Tofacitinib in AIA

C Tofacitinib in CIA

D Tofacitinib in CIA

Figure 5

Figure 6

Figure 7

A AIA - Indomethacin

E_{max}=58.5%
EC_{50}=0.646 μM
E=3.34 %×μM^{-1}

B AIA - Etanercept

E_{max}=24.6%
EC_{50}=1.46 μg/mL
E=0.246 %×μg^{-1}mL

C AIA - Tofacitinib

E_{max}=47.7%
EC_{50}=0.0726 μM
E=18.6 %×μM^{-1}

D CIA - Indomethacin

E_{max}=68.4%
EC_{50}=0.671 μM
E=2.03 %×μM^{-1}

E CIA - Etanercept

E_{max}=64.0%
EC_{50}=2.15 μg/mL

F CIA - Tofacitinib

E_{max}=105%
EC_{50}=0.0512 μM

Figure 8